

Align Yourself: Self-supervised Pre-training for Fine-grained Recognition via Saliency Alignment

Di Wu^{1,2*} Siyuan Li^{1,2*} Zelin Zang^{1,2} Kai Wang³ Lei Shang³
 Baigui Sun³ Hao Li³ Stan Z. Li^{1,2†}

¹AI Lab, School of Engineering, Westlake University;

²Institute of Advanced Technology, Westlake Institute for Advanced Study;

³Damo Academy, Alibaba Group;
 Hangzhou, Zhejiang, China

{wudi, lisiyuan, zangzelin, Stan.ZQ.Li}@westlake.edu.cn;
 {pusuan.wk, sl172005, baigui.sbg, lihao.lh}@alibaba-inc.com

Abstract

Self-supervised contrastive learning has demonstrated great potential in learning visual representations. Despite their success on various downstream tasks such as image classification and object detection, self-supervised pre-training for fine-grained scenarios is not fully explored. In this paper, we first point out that current contrastive methods are prone to memorizing background/foreground texture and therefore have a limitation in localizing the foreground object. Analysis suggests that learning to extract discriminative texture information and localization are equally crucial for self-supervised pre-training under fine-grained scenarios. Based on our findings, we introduce Cross-view Saliency Alignment (CVSA), a contrastive learning framework that first crops and swaps saliency regions of images as a novel view generation and then guides the model to localize on the foreground object via a cross-view alignment loss. Extensive experiments on four popular fine-grained classification benchmarks show that CVSA significantly improves the learned representation.

1 Introduction

Learning visual representations without supervision by leveraging pretext tasks has become increasingly popular. Various learning approaches such as colorization [41], spatial patch prediction [27], rotation [12] have been proposed to learn such representations. The objective of these pretext tasks is to capture invariant features through predicting transformations applied to different views of the same image.

More recently, self-supervised representation learning has witnessed significant progress by the use of contrastive loss [15, 25, 19, 16, 5]. Despite that contrastive-based methods have even outperformed supervised methods under some circumstances, their success has largely been confined to large-scale general-purpose datasets (coarse-grained) such as ImageNet [22]. Little to no effort has been made to adapt representations learned on coarse-grained settings to fine-grained settings utilizing unlabeled fine-grained datasets during pre-training. A substantial gap exists between self-supervised and supervised representation learning on fine-grained object recognition due to the subtle visual differences among different classes.

*These authors contribute equally to this work.

†Corresponding author.

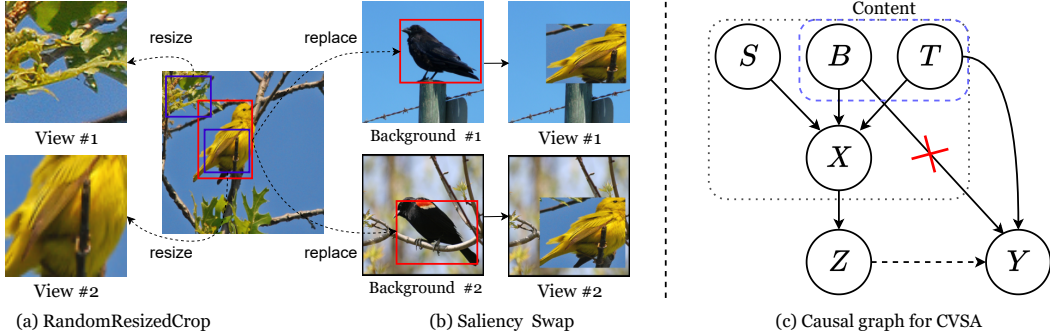


Figure 1: (a) illustrates the most commonly adopted *RandomResizedCrop* in current contrastive learning. The random cropping manner may cause two views to contain mainly the background of the image, which leads to semantic inconsistency between the views. (b) shows our proposed SaliencySwap. We crop from the region of interest from the reference image and replace the saliency regions of two randomly selected background images. Views generated with our method guarantees semantic information in different views. (c) interprets existing contrastive methods vs. CVSA from a causal perspective, the direct links denote the causalities between the two nodes: cause \rightarrow effect.

We argue that current contrastive learning methods only work on coarse-grained iconic images with large foreground objects residing in the background with informative discriminative texture (e.g., ImageNet [22]), but perform poorly when background texture provides little clue (e.g., CUB [34]) for fine-grained separation.

This paper analyzes and compares knowledge learned by various self-supervised methods and supervised methods during pre-training. We find that current self-supervised contrastive learning methods tend to learn low-level discriminative texture information and lack the localization ability of the foreground object. In contrast, the supervised method shows better localization ability. Specifically, we show that the incompetence of localization of current contrastive learning is primarily due to the commonly adopted *RandomResizedCrop* augmentation where a random size patch at a random location is cropped and resized to the original size. As illustrated in Fig. 1 (a), the model learns a semantic representation of the bird by contrasting the tree and the wing of the bird. This practice may be reasonable for coarse-grained recognition if background cues are more associated with the class than the foreground cues (e.g. $p(\text{bird}|\text{tree}) > p(\text{car}|\text{tree})$). However, the background of the image being a tree is not as informative when distinguishing bird species. Consequently, the model learns by cheating on picking low-level texture clues (usually from the background) instead of learning by localizing the foreground. This phenomenon is mutual for existing contrastive methods such as MoCo.v2[7], BYOL[14] and SimCLR[6] despite different contrastive mechanisms.

To mitigate the limitation of localization ability, we propose a pre-training framework called Cross-view Saliency Alignment (CVSA). CVSA consists of two algorithmic components: (a) A data augmentation strategy called SaliencySwap, which swaps the saliency region of the reference image with the saliency region of a randomly selected background image. A demonstration of SaliencySwap in comparison with *RandomResizedCrop* is shown in Fig. 1, and (b) an alignment loss that provides explicit localization supervision signal by forcing the model to give the highest correspondence response intensity of the foreground object across views. Our proposed augmentation ensures semantic consistency between augmented views while introduces background variation. Besides, SaliencySwap is a general plug-and-play augmentation strategy that could be used alongside existing contrastive methods.

On top of the proposed CVSA, to further bridge the performance gap between self-supervised and supervised representation learning on a fine-grained recognition problem, we offer a dual-stage pre-training pipeline that utilizes coarse-grained datasets ImageNet for low-level feature extraction and fine-grained datasets such as CUB for higher-level localization. In particular, we refer to the traditional contrastive learning methods such as MoCo.v2 and BYOL on ImageNet or COCO as the first stage and the proposed CVSA as the second stage.

In short, this paper makes the following contributions:

- We provide analysis of knowledge learned by various self-supervised methods compared to supervised methods during the fine-grained pre-training phase and point out the cause of limitation.
- We develop a novel contrastive learning framework for fine-grained recognition, which contains a data augmentation technique called *SaliencySwap* which guarantees semantic consistency between views and an *alignment objective* which enables the model to localize.
- We evaluate our approach and demonstrate its effectiveness on fine-grained benchmarks through extensive experiments.

2 Related Work

Self-supervised approaches have largely reduced the performance gap between supervised models and even achieved superior results on downstream vision tasks. Most early methods design handcrafted pretext tasks, such as relative patch prediction [11], colorization [42] and rotation prediction [13]. These pretext tasks rely on somewhat ad-hoc heuristics, which limits the generality of learned representations. Another popular form is clustering-based methods [3, 39, 2, 4]. More recently, contrastive learning [17, 6, 14] achieved state-of-the-art performance, which learns discriminative representations by contrasting positive pairs against negative pairs. For there are trivial solutions in these methods, such as a constant representation, different mechanisms [8, 37, 14] are proposed to learn useful representations.

Xiao *et al.* [31] propose to construct separate embedding sub-spaces for each augmentation instead of a single embedding for all augmentations. Their approach outperforms MoCo.v2[17] on downstream classification task on some fine-grained benchmarks. However, their method is trained on a general-purpose coarse-grained ImageNet dataset and makes no use of a fine-grained dataset during pre-training. In this work, we propose a dual-stage pre-training pipeline that utilizes coarse and fine-grained datasets for better fine-grained representation learning.

Current efforts [35, 30, 45, 20, 43] in fine-grained recognition are primarily dedicated to fine-tuning model pre-trained on supervised ImageNet either by localizing distinct parts[35, 30, 44, 10] or by fine-grained feature representation learning. However, there exists little exploration in self-supervised pre-training for fine-grained categorization. In the paper, we attempt to bring the localization and fine-grained feature representation learning to the pre-training stage, making use of fine-grained dataset.

3 What is Required for Fine-grained Pre-training?

We attempt to answer the proposed question by evaluating the capabilities learned out of three classes of pre-training methods, namely self-supervised contrastive, non-contrastive methods, and supervised methods. In particular, we focus on two main capabilities: discriminative feature extraction ability and localization ability. Without loss of generality, we select MoCo.v2, BYOL, supervised ResNet, and rotation for comparison. In addition, we develop a simple binary classification as a pre-training task. During pre-training, the model is asked to classify images from CUB as foreground class and images from COCO as background class.

3.1 Experimental Setup

Dataset. We evaluate the performance of baselines’ representation after pre-training on the training set of 100 % IN, 10 % IN, COCO, and CUB, details of datasets used are described in Sec. 5. We use the same fixed split for the 10 % IN where we randomly sample 10 % of the total training set size from each class.

Pre-training Details. To ensure impartial comparisons, we use the data augmentations described in [7] for both MoCo.v2 and BYOL. For rotation, we follow the exact setup as described in the original paper. For the binary classification, We pre-train the model for 800 epochs with an SGD optimizer with an initial learning rate of 0.1 with cosine annealing, weight decay, and momentum is set to $1e - 4$ and 0.9, respectively.

Evaluations. We first evaluate the performance obtained when fine-tuning learned representation on a classification task on CUB training set with label information by training a linear classifier on

| Method | 100% IN | | | 10% IN | | | COCO | | | CUB | | |
|------------|--------------|--------------|--------------|--------------|--------------|--------------|--------------|--------------|--------------|--------------|--------------|--------------|
| | Semi | Linear | WSOL |
| PyTorch SL | 79.25 | 67.64 | 49.73 | 74.68 | 63.07 | 48.83 | - | - | - | 55.51 | 5.85 | 30.31 |
| Rotation | 67.66 | 25.29 | 46.13 | 69.64 | 23.71 | 47.07 | 67.95 | 16.57 | 43.53 | 67.33 | 15.46 | 34.69 |
| MoCo.v2 | 69.99 | 33.33 | 47.59 | 69.62 | 25.32 | 51.12 | 68.69 | 18.69 | 48.12 | 61.82 | 15.03 | 33.36 |
| BYOL | 72.61 | 27.17 | 50.15 | 70.42 | 20.38 | 46.55 | 70.09 | 16.45 | 45.96 | 63.65 | 15.14 | 33.81 |

Table 1: **Comparison of pre-training methods.** Top-1 accuracy (in %) under semi-supervised and linear evaluation is reported. For the task of WSOL, we report MaxBoxAcc.

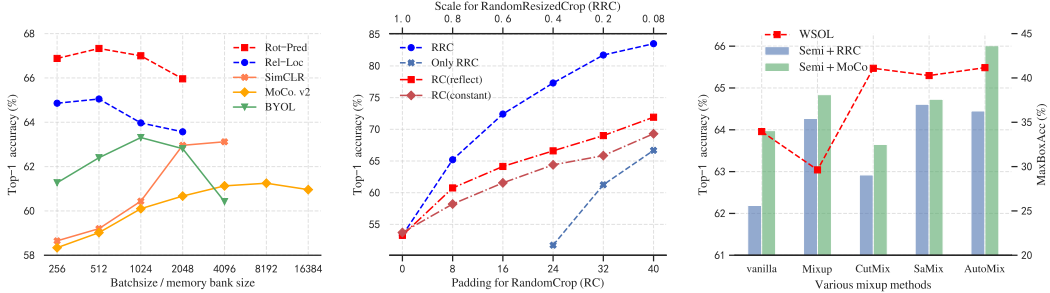


Figure 2: (a) Analysis of the batch size or memory bank size of various self-supervised methods. (b) The horizontal axis on the top indicates the scale factor in *RandomResizedCrop* (RRC) while the bottom axis indicates various padding sizes for *RandomCrop* (RC) with two padding modes. The top-1 accuracy (in %) under semi-supervised evaluation is reported. Notice that RRC outperforms RC with different padding modes, and only using RRC is still outperforms only without RRC, which shows that RRC is essential to contrastive learning. (c) Performance analysis of foreground-background classification under different augmentations.

top of the frozen representation, following the procedure described in [5][28][42]. We refer to the linear test accuracy with self-supervised pre-training as the model’s discriminative feature extraction ability. We then perform a semi-supervised test following the protocol of [38][5]. This time the whole network is fine-tuned using the CUB training set. We refer to the semi-supervised protocol as the pre-training representation quality metric for fine-grained classification problems. Since we use CUB instead of IN during a linear and semi-supervised test, we describe the deviation from the original protocols as follows. We use the SGD optimizer with the initial learning rate with cosine annealing, and momentum is set as 0.9. A batch size of 16 and a fixed training epoch of 50 are adopted. We sweep over the learning rate $\{0.1, 0.05, 0.01, 0.005, 0.001\}$ and weight decay $\{5e-4, 1e-4\}$ and select the hyperparameters achieving the best performance on validation set to report top-1 accuracy on the test set. To evaluate the localization ability of different approaches, we use a class activation mapping (CAM) based metric called MaxBoxAcc described in [9]. A larger MaxBoxAcc indicates better localization ability.

3.2 Essential Requirement and Formulation

Where does the gap lie between self-supervised and supervised pre-training? We first compare supervised and self-supervised methods. Results are shown in Table 1. Compared to supervised pre-training, all three self-supervised approaches yield lower MaxBoxAcc, indicating a lack of localization ability. This is not surprising because self-supervised methods are task-agnostic and could only learn low-level features, i.e., gradient and direction-dependent features for rotation, invariant features across views to cluster different objects for contrastive methods. However, the supervised method discards task-irrelevant information and extracts related semantic features. We also observe that there exists a positive correlation between semi-supervised accuracy and the MaxBoxAcc. This enlightens us that localization ability is crucial for fine-grained pre-training.

Why doesn’t contrastive method look at the bird? We hypothesize that the lack of localization ability comes from the commonly adopted *RandomResizedCrop* augmentation, where a random size patch at the random location is cut from the original image and then resized to the original size. When asked to pull together two patches cut from the same image, models often cheat by exploiting low-level texture features. We show in Fig. 2 (b) that the performance of BYOL drops drastically

as the cropped patch scale enlarges on the STL-10 dataset. The best accuracy is achieved with a scaling factor of 0.08, which is the default hyperparameter choice for current contrastive learning approaches. Contrasting overly small patches forces the model to extract local texture features and lack localization ability. We formulate current contrastive methods with a causal graph as illustrated in Fig. 1 (c). Let X be images with content composed of background prior B and foreground target prior T , generated with style prior S as augmentations like color jittering. Latent representation Z is learned and used to infer image labels Y . Contrastive methods assume image labels Y are an effect of both B and T (all image content) due to the local texture-biased nature. Also, Table 1 shows that self-supervised methods give higher semi-supervised accuracy on larger datasets such as IN and COCO. Figure 2 (a) shows that the hand-craft methods yield better representation than contrastive-based algorithms on CUB. These indicate that the performance of low-level feature extraction is related to the size of the dataset.

Is Localization All You Need? To answer this question, We report linear and semi-supervised test accuracy as well as MaxBoxAcc of the binary classification on the CUB test set with different mixup augmentations[40, 32, 24, 36] as well as image augmentations in Fig. 2 (c). It is observed that the binary classification pre-training yields similar MaxBoxAcc as supervised pre-training, yet there still exists a vast semi-supervised accuracy gap. We assume that the gap comes from an inferior feature extraction ability of the binary classification pre-training, as could be conducted from a much lower linear test accuracy. In other words, discriminative feature extraction ability is as essential as localization ability. Besides, mixup augmentation gives better localization ability and, as a consequence, higher Semi-supervised accuracy. While *RandomResizedCrop* leads to the lack of localization ability, we address this problem by proposing an image augmentation technique that swaps saliency regions of images.

From the previous analysis, given a fine-grained classification problem, similar to [1], we assume an underlying set of discrete latent classes \mathcal{C} that represent semantic content, we obtain the joint distribution:

$$p(c, x) = p(c|x_f) \cdot p(x_f|x), \quad (1)$$

where x_f stands for the foreground object. This factorization captures two important intuitions: (1) Given an image of a fine-grained object; the model should first localize the foreground object, namely, the localization ability of the model. (2) To further tell the species of the foreground object, discriminative texture features should be extracted, namely, the texture extraction ability of the model. Following this formulation, a dual-stage pre-training pipeline is naturally proposed for self-supervised fine-grained recognition. The model’s discriminative texture extraction ability could be fulfilled by first-stage pre-training on large datasets such as ImageNet. In the first stage, we regard the image content as a whole as the same assumption of current contrastive methods. For the second-stage pre-training, we propose a framework called Cross-view Saliency Alignment (CVSA), attempting to break the causality between B and Y by enabling the model’s localization capability.

4 Cross-view Saliency Alignment

In this section, we formalize the proposed CVSA framework, as illustrated in Fig. 3. We first introduce an image augmentation strategy in Sec. 4.1 called SaliencySwap in replacement of previous commonly used *RandomResizedCrop* in contrastive learning. This augmentation introduces background variance and forces the network to extract features mainly from the less variant foreground(saliency region). Subsequently, in Sec. 4.2 we wish to improve further the localization ability of self-supervised model under fine-grained setting by applying an alignment loss on representations at different granularity levels across views.

4.1 SaliencySwap

The purpose of SaliencySwap is to maximally utilize the saliency information for foreground semantic consistency between two views of the same image while introducing background variation. Unlike *RandomResizedCrop*, our method guarantees that each view at least contains part of the foreground object and thus prevents the backbone from learning irrelevant feature representation through pure background information. Besides, we swap the saliency region from the source image and the saliency region from another randomly selected image to avoid saliency ambiguity. After swapping,

the backbone is thus forced to extract object-oriented saliency features from the common saliency region instead of the random background. Here we explain the process in detail.

4.1.1 Source Saliency Detection

A saliency detection algorithm generates a saliency map, usually in the form of intensity, which indicates the objects of interest and thereby primarily focuses on the foreground. Let $I \in \mathbb{R}^{W \times H \times C}$ be an image in the training set, define f to be a saliency detection algorithm, then the output saliency map $S_{i,j} = f(I_{i,j}) \in \mathbb{R}^{W \times H}$ indicates the saliency intensity value at pixel $I_{i,j}$. The saliency information can be noisy. Therefore, we seek to find a bounding box $B = (l, t, W_b, H_b)$ of the foreground object with highest averaged saliency information satisfying the following objective function:

$$\operatorname{argmax}_{W_b, H_b, l, t} \sum_{i=l}^{i=l+W_b} \sum_{j=t}^{j=t+H_b} \frac{S_{i,j}}{W_b \times H_b}. \quad (2)$$

A corresponding binary saliency mask $M \in \mathbb{R}^{W \times H}$ is defined by filling with 0 within the bounding box B , otherwise 1. Then we select a random patch within the bounding box B as the foreground. This ensures that the patch cropped contains information mainly of the foreground, not the background. Similar to *RandomResizedCrop*, the size of the patch is determined based on an area ratio (to the area of the bounding box), which is sampled from a uniform distribution $unif(\lambda, 1)$.

4.1.2 Foreground Background Fusion

We then combine the selected foreground patch from the source image (foreground image) with another randomly selected image (background image). To avoid saliency ambiguity where the augmented images are composed of multiple semantic objects, our approach restricts each augmented view to contain the saliency information only of one object of the desired fine-grained class. Here we consider two ways of merging based on different choices of the background dataset. (I) The background dataset is the same as the foreground dataset. The background image contains an object of the same desired fine-grained class. Therefore, the saliency information of the background needs to be eliminated. We first calculate the bounding box B_f , B_b of the foreground and background, respectively, using equation 2. Then select a random patch from the foreground B_f and resize it to the shape of B_b . Finally, we replace B_b with the resized foreground patch. (II) The background dataset is different from the foreground dataset. To avoid the background from having an object of the same fine-grained class as the foreground. We wish the background dataset to be rich in different environments. Thus we choose dataset like COCO [23] and avoid dataset like ImageNet[22] which has large foreground wrt background. Again, we first calculate the bounding box B_f of the foreground and select a random patch. Then we resize the selected patch based on an area ratio (to the area of the background) which is sampled from a uniform distribution $(\beta, 1)$. Finally, we "paste" the resized patch to a random location in the background.

4.2 Cross-view Saliency Alignment Module

Given two views I_q and I_k of Image I augmented by a pipeline containing SaliencySwap and other augmentation operations such as random flipping and color jittering. Define M_k and M_q to be their saliency mask, respectively. Let f_q^l and $f_k^l \in \mathbb{R}^{W^l \times H^l, C^l}$ be the C^l dimensional $H^l \times W^l$ feature planes encoded by an encoder network $f = \phi(I)$ consisting of a backbone (e.g., ResNet [18]), which is truncated at stage l and a projection MLP head [6]. Following BYOL[14], a prediction MLP head h is adopted to match the output of one view and match it to the other. In addition, we propose a saliency alignment module that contains a convolution-based head g for saliency alignment. The overall framework is illustrated in Fig. 3 (b).

Cross-view Attention. We seek to capitalize on the pixel-level foreground interactions between the feature maps of two different augmented views. We first build a cross-view attention map:

$$A_{q \rightarrow k}^l = g(f_q^l) * f_k^l^T, \quad (3)$$

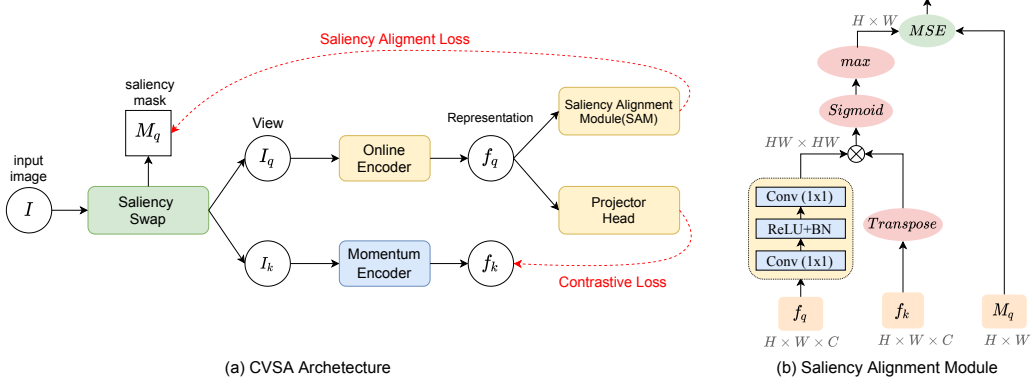


Figure 3: Conceptual illustration of learning paradigm of Cross-view Saliency Alignment.

where $g(\cdot)$ is the alignment prediction head, T denotes matrix transposition. The location-aware attention map $A^l \in R^{W^l \times H^l, W^l * H^l}$ then indicates a pair-wise spatial correspondence between any pixel from $g(f_q^l)$ and any pixel from f_k^l .

Joint Saliency Alignment. The proposed SaliencySwap ensures that the feature map of each view contains features extracted from the foreground object. To further enhance the backbone’s ability to identify the location of the foreground object, we propose to align the saliency mask with the pixels from its corresponding feature map with the highest correspondence intensity against the other. The correspondence intensity C could be found as:

$$C_{q \rightarrow k} = \text{res}(\max(\sigma(A_{q \rightarrow k}))), \quad (4)$$

where σ is the sigmoid function, $\text{res} : R^{W^l \times H^l, 1} \rightarrow R^{W^l, H^l}$ denotes the reshaping operation of the matrix. Note that the \max operation is taken over the second axis of A . We then define a symmetrized alignment loss between the saliency mask M and the correspondence intensity matrix C :

$$\mathcal{L}_{align} = \sum_l \left\| \delta^l(M_q) - C_q^l \right\|^2 + \left\| \delta^l(M_k) - C_k^l \right\|^2, \quad (5)$$

where $\delta^l : R^{W \times H} \rightarrow R^{W^l \times H^l}$ denotes the bilinear pooling operation. The proposed alignment loss restricts the most cross view correlated pixels to the saliency region and thus gives the model localization ability. In addition, different network layers present object semantics in different scales, where the latter one has a larger receptive field. Leveraging cross-layer semantics also enhances the representation of multi-scale learning.

Joint Objective. Following [8], we denote two output vectors as $p_q \stackrel{\text{def}}{=} h(\phi(I_q))$ and $f_k \stackrel{\text{def}}{=} \phi(I_q)$. We define a contrastive loss $\mathcal{L}_{contrast}$ using symmetrized negative cosine similarity $\mathcal{D}(p_q, f_k)$ of the two vectors as:

$$\mathcal{L}_{contrast} = \frac{1}{2} \mathcal{D}(p_q, f_k) + \frac{1}{2} \mathcal{D}(p_k, f_q), \quad \mathcal{D}(p_q, f_k) = -\frac{p_q}{\|p_q\|_2} \cdot \frac{f_k}{\|f_k\|_2}. \quad (6)$$

The joint objective used for the second-stage pretext task is defined as:

$$\mathcal{L} = \mathcal{L}_{contrast} + \mathcal{L}_{align}. \quad (7)$$

5 Experiments

In this section, we empirically study the effectiveness of our proposed CVSA framework for fine-grained pre-training and dual-stage pre-training pipelines.

5.1 Experimental settings

Implementation details. The encoder ϕ consists of a ResNet-50 network [18] followed by a three linear layer projector network. The first two linear layers are followed by ReLU and a batch normalization layer. The prediction head h has the same architecture as the projector network except for using different output units. We follow the exact experimental setup in [14] during the first stage of training. For the second stage CVSA, the alignment prediction head g consists of two 1×1 convolution layers with ReLU and batch normalization layer in between. We grid search cropping scale ratio of SaliencySwap $\lambda \in \{0.08, 0.2, 0.5, 0.8\}$. We use a learning rate of $lr \times \text{BatchSize}/256$ with $\text{BatchSize} = 1024$ and a base $lr \in \{0.3, 0.6, 0.9, 1.2\}$. For image augmentations, we replace *RandomResizedCrop* with our proposed SaliencySwap and use the same all other augmentations described in Sec. 3. For simplicity, we use the ground truth bounding box of each dataset due to most detectors are trained in a supervised manner. For the dual-stage pre-training, we initialize the second stage network with the weight pre-trained on the first stage and freeze the first two blocks of the ResNet backbone. We use the same setup as in Sec. 3 for all other unstated setups.

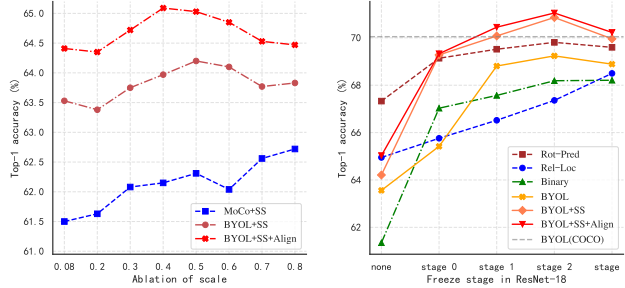


Figure 4: Hyperparameter ablation of SaliencySwap and freeze stage ablation of the dual-stage pipeline. The dotted grey line on the right indicates the performance of first-stage training of BYOL on COCO.

| bg dataset | BYOL | +SS | +SS+Al |
|------------|-------|-------|--------|
| (CUB) | 63.14 | 64.35 | 65.02 |
| +COCO | 59.96 | 61.18 | 61.73 |
| +NAbirds | 63.31 | 63.77 | 64.80 |

Table 2: **Background dataset evaluation for second stage pre-training.** We evaluate the effect of different background fusion methods proposed in Sec. 4 on CUB. Top-1 accuracy (in %) under semi-supervised evaluation is reported. SS denotes using the SaliencySwap, and Al denotes using the alignment loss.

| Methods | Stage-1 | Stage-2 | CUB | NAbirds | Aircrafts | Cars |
|---------------|----------|---------|------------------------|------------------------|------------------------|------------------------|
| BYOL[14] | - | ✓ | 64.85 (+0.00) | 72.54 (+0.00) | 70.36 (+0.00) | 75.87 (+0.00) |
| BYOL+SS+Align | - | ✓ | 66.69 (+1.84) | 73.49 (+3.13) | 73.22 (+2.86) | 77.31 (+1.44) |
| MoCo.v2[7] | COCO2017 | - | 68.47 (-0.08) | 72.53 (-3.76) | 81.76 (+0.03) | 86.08 (-0.28) |
| BYOL[14] | COCO2017 | - | 68.55 (+0.00) | 76.29 (+0.00) | 81.73 (+0.00) | 86.36 (+0.00) |
| BYOL[14] | COCO2017 | ✓ | 68.10 (-0.45) | 75.82 (-0.47) | 80.53 (-1.20) | 85.58 (-0.78) |
| BYOL+SS+Align | COCO2017 | ✓ | 69.07 (+0.52) | 77.57 (+1.28) | 82.67 (+0.94) | 87.13 (+0.77) |
| Supervised | 100% IN | - | 81.02 (+4.39) | 80.09 (+1.20) | 87.25 (+0.06) | 90.61 (+1.02) |
| SimCLR[5] | 100% IN | - | 73.99 (-2.64) | 76.30 (-2.59) | 85.96 (-1.23) | 88.16 (-1.43) |
| MoCo.v2[7] | 100% IN | - | 73.19 (-3.44) | 75.64 (-3.25) | 85.49 (-1.70) | 87.41 (-2.18) |
| BYOL[14] | 100% IN | - | 76.63 (+0.00) | 78.89 (+0.00) | 87.19 (+0.00) | 89.59 (+0.00) |
| BYOL+SS+Align | 100% IN | ✓ | 76.75 (+0.08) | 79.38 (+0.49) | 87.23 (+0.04) | 89.48 (-0.11) |

Table 3: **CVSA vs. other pre-training methods on fine-grained benchmarks.** Dataset name in column Stage-1 indicates dataset used, otherwise not performed. ✓: second stage pre-training performed on corresponding fine-grained dataset. Top-1 accuracy (in %) under semi-supervised evaluation is reported. Text in grey indicates baseline while green suggests improvement over baseline and red for degradation. SS stands for SaliencySwap and Align for the proposed alignment loss.

Dataset. In this paper, we assess the performance of the representation pre-trained using dual-stage, first-stage only and second-stage only on four public popular benchmarks: 1) CUB-200-2011 [34] contains 11,788 images from 200 wild bird species, which is the widely-used benchmark for its representativeness, 2) Stanford-Cars [21] contains 16,185 images of 196 car subcategories, 3) FGVC-Aircraft [26] contains 10,000 images of 100 classes of aircrafts and 4) NA-birds [33] is a large dataset with 48,562 images for over 555 bird classes. We follow the standard dataset partition as in the original works. For first-stage pre-training, we adopt two popular vision benchmarks: 1) ImageNet contains 1000 different classes of iconic images of the training set size of 1,281,167. 2) COCO contains 118,000 images with much more complex scenes of many objects.

5.2 Comparison with State-of-the-art

For comparison, in Table 3, we report the classification Top-1 accuracy on the test set of the fine-grained dataset using semi-supervised test protocol the same way as described in Sec. 3. Since our approach extends BYOL, we choose BYOL as the baseline for pre-training using different stages and datasets. We also include supervised-pretraining denoted as Supervised. When applying only the second-stage training, namely pre-training using the training set of the fine-grained datasets from scratch, our proposed CVSA outperforms BYOL by a large margin on all four benchmarks. When applying the dual-stage pre-training using COCO for the first-stage pre-training, our proposed method shows a consistent improvement on representations learned during the first stage. However, the improvement of CVSA when using IN for the first-stage pre-training is not as significant on Aircraft and Cars. We hypothesize that this is due to the iconic nature of these two datasets. We observe that most images of these two datasets are of similar and straightforward background, restricting our proposed SaliencySwap. Besides, Table 3 suggests that the accuracy pre-trained on the first stage is higher than pre-trained on the second stage for all methods. This is consistent with our formulation in Sec. 3 that discriminative feature extraction relies on the size of the dataset, and localization ability alone is not enough for fine-grained recognition. It is noted from Table 3 that when applying dual-stage pre-training, our method outperforms both BYOL and MoCo.v2 pre-trained on the same dataset with the first stage. This indicates that our proposed pre-training pipeline improves learned representation for fine-grained downstream classification.

5.3 Ablation Study

Module Effectiveness Ablation. We demonstrate the effectiveness of our CVSA innovations by adding them one by one onto the baseline. We first validate our proposed augmentation SaliencySwap. We compare the performance of MoCo.v2 and BYOL using SaliencySwap with *RandomResizedCrop* while keeping all other augmentations the same as in [7]. We report results in the top-1 accuracy on the CUB test set under semi-supervised protocol as in Sec. 3 using ResNet18 as the backbone. As can be seen from Fig. 4, SaliencySwap as an augmentation outperforms *RandomResizedCrop* both for MoCo.v2 and BYOL. We then add cross-view saliency alignment loss onto BYOL using SaliencySwap. We observe a further accuracy improvement. Now, we have shown that both SaliencySwap and alignment loss contribute to higher performance.

Hyperparameter Ablation. We then compare the performance of SaliencySwap using different crop scaling hyperparameter, specifically $\lambda \in \{0.08, 0.2, 0.3, 0.4, 0.5, 0.8\}$ in Fig. 4. From Fig. 2 (b), the performance of BYOL fluctuates drastically under the different scaling factor of *RandomResizedCrop* and the best result is achieved with a scaling factor being 0.08. However, BYOL yields similar performance under different choices of λ . We argue that SaliencySwap, together with alignment loss, helps the model to localize on the foreground object, and thus local texture is no longer the only clue for contrastive pre-training to learn representation. Then, we study the effect when freezing different stages of the ResNet18 backbone in the second stage pre-training. We initialize the second-stage backbone with the weights pre-trained on COCO using BYOL(first-stage). Again, We give top-1 accuracy under semi-supervised protocol on CUB in Fig. 4. The horizontal axis indicates freezing up to different stages of ResNet. The highest accuracy is achieved when freezing up to the second stage of ResNet for all methods. We hypothesize that the early stages of ResNet mostly extract low-level texture information and later stages for higher-level features such as localization. Intuitively, we wish to enhance the model’s localization ability without jeopardizing the texture extraction ability acquired during the first stage. This explains the reason for freezing up to the second stage during the second stage, which is a common practice in the detection domain[29]. Lastly, we compare different foreground-background fusion methods proposed in Sec. 4 and give result in Table 2.

6 Conclusion

We first investigate the cause of the performance gap between supervised and self-supervised pre-training for fine-grained recognition in this work. We point out that the model’s localization ability and discriminative feature extraction ability are equally important. Under this formulation, We propose a dual-stage pre-training with the first stage to train feature extraction and the second stage to train localization. To better help the model localize, we propose *Cross-view Saliency Alignment*, a new unsupervised contrastive representation learning framework. Extensive experiments

on popular fine-grained benchmarks demonstrate the effectiveness of our contributions in learning better representation for fine-grained recognition. Future work includes investigating combining the dual-stage training process to a single-stage framework.

References

- [1] Sanjeev Arora, Hrishikesh Khandeparkar, Mikhail Khodak, Orestis Plevrakis, and Nikunj Saunshi. A theoretical analysis of contrastive unsupervised representation learning. *International Conference on Machine Learning*, 2019.
- [2] Yuki Markus Asano, Christian Rupprecht, and Andrea Vedaldi. Self-labelling via simultaneous clustering and representation learning. In *International Conference on Learning Representations (ICLR)*, 2020.
- [3] Mathilde Caron, Piotr Bojanowski, Armand Joulin, and Matthijs Douze. Deep clustering for unsupervised learning of visual features. In *Proceedings of the European Conference on Computer Vision (ECCV)*, 2018.
- [4] Mathilde Caron, Ishan Misra, Julien Mairal, Priya Goyal, Piotr Bojanowski, and Armand Joulin. Unsupervised learning of visual features by contrasting cluster assignments. In *Advances in Neural Information Processing Systems (NeurIPS)*, 2020.
- [5] Ting Chen, Simon Kornblith, Mohammad Norouzi, and Geoffrey Hinton. A simple framework for contrastive learning of visual representations. *arXiv preprint arXiv:2002.05709*, 2020.
- [6] Ting Chen, Simon Kornblith, Mohammad Norouzi, and Geoffrey Hinton. A simple framework for contrastive learning of visual representations. *arXiv preprint arXiv:2002.05709*, 2020.
- [7] Xinlei Chen, Haoqi Fan, Ross Girshick, and Kaiming He. Improved baselines with momentum contrastive learning. *arXiv preprint arXiv:2003.04297*, 2020.
- [8] Xinlei Chen and Kaiming He. Exploring simple siamese representation learning. In *Proceedings of the Conference on Computer Vision and Pattern Recognition (CVPR)*, 2021.
- [9] Junsuk Choe, Seong Joon Oh, Seungho Lee, Sanghyuk Chun, Zeynep Akata, and Hyunjung Shim. Evaluating weakly supervised object localization methods right. In *Conference on Computer Vision and Pattern Recognition (CVPR)*, 2020.
- [10] Yao Ding, Yanzhao Zhou, Yi Zhu, Qixiang Ye, and Jianbin Jiao. Selective sparse sampling for fine-grained image recognition. In *Proceedings of the International Conference on Computer Vision (ICCV)*, pages 6599–6608, 2019.
- [11] Carl Doersch, Abhinav Gupta, and Alexei A Efros. Unsupervised visual representation learning by context prediction. In *Proceedings of the International Conference on Computer Vision (ICCV)*, 2015.
- [12] Spyros Gidaris, Praveer Singh, and Nikos Komodakis. Unsupervised representation learning by predicting image rotations. *International Conference on Learning Representations*, 2018.
- [13] Spyros Gidaris, Praveer Singh, and Nikos Komodakis. Unsupervised representation learning by predicting image rotations. In *International Conference on Learning Representations (ICLR)*, 2018.
- [14] Jean-Bastien Grill, Florian Strub, Florent Altché, Corentin Tallec, Pierre H Richemond, Elena Buchatskaya, Carl Doersch, Bernardo Avila Pires, Zhaohan Daniel Guo, Mohammad Gheshlaghi Azar, et al. Bootstrap your own latent: A new approach to self-supervised learning. In *NeurIPS*, 2020.
- [15] Raia Hadsell, Sumit Chopra, and Yann LeCun. Dimensionality reduction by learning an invariant mapping. In *2006 IEEE Computer Society Conference on Computer Vision and Pattern Recognition (CVPR’06)*, volume 2, pages 1735–1742. IEEE, 2006.
- [16] Kaiming He, Haoqi Fan, Yuxin Wu, Saining Xie, and Ross Girshick. Momentum contrast for unsupervised visual representation learning. *Proceedings of the IEEE conference on computer vision and pattern recognition*, 2020.
- [17] Kaiming He, Haoqi Fan, Yuxin Wu, Saining Xie, and Ross Girshick. Momentum contrast for unsupervised visual representation learning. In *Proceedings of the Conference on Computer Vision and Pattern Recognition (CVPR)*, 2020.
- [18] Kaiming He, Xiangyu Zhang, Shaoqing Ren, and Jian Sun. Deep residual learning for image recognition. In *Proceedings of the IEEE conference on computer vision and pattern recognition*, pages 770–778, 2016.

- [19] Olivier J Hénaff, Aravind Srinivas, Jeffrey De Fauw, Ali Razavi, Carl Doersch, SM Eslami, and Aaron van den Oord. Data-efficient image recognition with contrastive predictive coding. *arXiv preprint arXiv:1905.09272*, 2019.
- [20] Zixuan Huang and Yin Li. Interpretable and accurate fine-grained recognition via region grouping. In *Proceedings of the Conference on Computer Vision and Pattern Recognition (CVPR)*, pages 8662–8672, 2020.
- [21] Jonathan Krause, Michael Stark, Jia Deng, and Li Fei-Fei. 3d object representations for fine-grained categorization. In *Proceedings of the IEEE International Conference on Computer Vision Workshops*, pages 554–561, 2013.
- [22] Alex Krizhevsky, Ilya Sutskever, and Geoffrey E Hinton. Imagenet classification with deep convolutional neural networks. In *Advances in neural information processing systems*, pages 1097–1105, 2012.
- [23] Tsung-Yi Lin, Michael Maire, Serge Belongie, James Hays, Pietro Perona, Deva Ramanan, Piotr Dollár, and C Lawrence Zitnick. Microsoft coco: Common objects in context. In *Proceedings of the European Conference on Computer Vision (ECCV)*, 2014.
- [24] Zicheng Liu, Siyuan Li, Di Wu, Zhiyuan Chen, Lirong Wu, Jianzhu Guo, and Stan Z. Li. Automix: Unveiling the power of mixup, 2021.
- [25] Lajanugen Logeswaran and Honglak Lee. An efficient framework for learning sentence representations. In *International Conference on Learning Representations*, 2018.
- [26] Subhransu Maji, Esa Rahtu, Juho Kannala, Matthew Blaschko, and Andrea Vedaldi. Fine-grained visual classification of aircraft. *arXiv preprint arXiv:1306.5151*, 2013.
- [27] Mehdi Noroozi and Paolo Favaro. Unsupervised learning of visual representations by solving jigsaw puzzles. In *European Conference on Computer Vision*, pages 69–84. Springer, 2016.
- [28] Aaron van den Oord, Yazhe Li, and Oriol Vinyals. Representation learning with contrastive predictive coding. *arXiv preprint arXiv:1807.03748*, 2018.
- [29] Shaoqing Ren, Kaiming He, Ross Girshick, and Jian Sun. Faster r-cnn: Towards real-time object detection with region proposal networks. In C. Cortes, N. Lawrence, D. Lee, M. Sugiyama, and R. Garnett, editors, *Advances in Neural Information Processing Systems*, volume 28. Curran Associates, Inc., 2015.
- [30] Marcel Simon and Erik Rodner. Neural activation constellations: Unsupervised part model discovery with convolutional networks. In *Proceedings of the International Conference on Computer Vision (ICCV)*, pages 1143–1151, 2015.
- [31] Xiao Tete, Wang Xiaolong, A. Efros Alexei, and Darrell Trevor. What should not be contrastive in contrastive learning, 2021.
- [32] AFM Uddin, Mst Monira, Wheemyung Shin, TaeChoong Chung, Sung-Ho Bae, et al. Saliencymix: A saliency guided data augmentation strategy for better regularization. *arXiv preprint arXiv:2006.01791*, 2020.
- [33] Grant Van Horn, Steve Branson, Ryan Farrell, Scott Haber, Jessie Barry, Panos Ipeirotis, Pietro Perona, and Serge Belongie. Building a bird recognition app and large scale dataset with citizen scientists: The fine print in fine-grained dataset collection. In *Proceedings of the Conference on Computer Vision and Pattern Recognition (CVPR)*, pages 595–604, 2015.
- [34] Catherine Wah, Steve Branson, Peter Welinder, Pietro Perona, and Serge Belongie. The caltech-ucsd birds-200-2011 dataset. 2011.
- [35] Tianjun Xiao, Yichong Xu, Kuiyuan Yang, Jiaxing Zhang, Yuxin Peng, and Zheng Zhang. The application of two-level attention models in deep convolutional neural network for fine-grained image classification. In *Proceedings of the Conference on Computer Vision and Pattern Recognition (CVPR)*, pages 842–850, 2015.
- [36] Sangdoo Yun, Dongyoon Han, Seong Joon Oh, Sanghyuk Chun, Junsuk Choe, and Youngjoon Yoo. Cutmix: Regularization strategy to train strong classifiers with localizable features. In *Proceedings of the IEEE/CVF International Conference on Computer Vision*, pages 6023–6032, 2019.
- [37] J. Zbontar, J. Li, I. Misra, Y Lecun, and S. Deny. Barlow twins: Self-supervised learning via redundancy reduction. *arXiv preprint arXiv:2103.03230*, 2021.

- [38] Xiaohua Zhai, Avital Oliver, Alexander Kolesnikov, and Lucas Beyer. S4l: Self-supervised semi-supervised learning. In *Proceedings of the IEEE international conference on computer vision*, pages 1476–1485, 2019.
- [39] Xiaohang Zhan, Jiahao Xie, Ziwei Liu, Yew Soon Ong, and Chen Change Loy. Online deep clustering for unsupervised representation learning. In *Proceedings of the Conference on Computer Vision and Pattern Recognition (CVPR)*, 2020.
- [40] Hongyi Zhang, Moustapha Cisse, Yann N Dauphin, and David Lopez-Paz. mixup: Beyond empirical risk minimization. *arXiv preprint arXiv:1710.09412*, 2017.
- [41] Richard Zhang, Phillip Isola, and Alexei A Efros. Colorful image colorization. In *European conference on computer vision*, pages 649–666. Springer, 2016.
- [42] Richard Zhang, Phillip Isola, and Alexei A Efros. Colorful image colorization. In *Proceedings of the European Conference on Computer Vision (ECCV)*, 2016.
- [43] Yifan Zhao, Ke Yan, Feiyue Huang, and Li Jia. Graph-based high-order relation discovery for fine-grained recognition. In *IEEE Conference on Computer Vision and Pattern Recognition (CVPR)*, 2021.
- [44] Heliang Zheng, Jianlong Fu, Tao Mei, and Jiebo Luo. Learning multi-attention convolutional neural network for fine-grained image recognition. In *Proceedings of the International Conference on Computer Vision (ICCV)*, pages 5209–5217, 2017.
- [45] Heliang Zheng, Jianlong Fu, Zheng-Jun Zha, and Jiebo Luo. Looking for the devil in the details: Learning trilinear attention sampling network for fine-grained image recognition. In *Proceedings of the Conference on Computer Vision and Pattern Recognition (CVPR)*, pages 5012–5021, 2019.